Top-interface-controlled fatigue of epitaxial $Pb(Zr_{0.52}Ti_{0.48})O_3$ ferroelectric thin films on $La_{0.7}Sr_{0.3}MnO_3$ electrodes

Wenbin Wu, K. H. Wong, C. L. Choy, and Y. H. Zhang

View Online   Export Citation

ARTICLES YOU MAY BE INTERESTED IN

Ferroelectric thin films: Review of materials, properties, and applications
Journal of Applied Physics **100**, 051606 (2006); https://doi.org/10.1063/1.2336999

Strain-dependent magnetic phase diagram of epitaxial $La_{0.67}Sr_{0.33}MnO_3$ thin films
Applied Physics Letters **76**, 2421 (2000); https://doi.org/10.1063/1.126363

Polarization fatigue in ferroelectric films: Basic experimental findings, phenomenological scenarios, and microscopic features
Journal of Applied Physics **90**, 1387 (2001); https://doi.org/10.1063/1.1381542

Top-interface-controlled fatigue of epitaxial Pb(Zr$_{0.52}$Ti$_{0.48}$)O$_3$ ferroelectric thin films on La$_{0.7}$Sr$_{0.3}$MnO$_3$ electrodes

Wenbin Wu[a)]
Structure Research Laboratory, University of Science and Technology of China, Hefei 230026, China and Department of Applied Physics, The Hong Kong Polytechnic University, Kowloon, Hong Kong, China

K. H. Wong and C. L. Choy
Department of Applied Physics, The Hong Kong Polytechnic University, Kowloon, Hong Kong, China

Y. H. Zhang
Structure Research Laboratory, University of Science and Technology of China, Hefei 230026, China

Epitaxial Pb(Zr$_{0.52}$Ti$_{0.48}$)O$_3$/La$_{0.7}$Sr$_{0.3}$MnO$_3$(PZT/LSMO) and LSMO/PZT/LSMO heterostructures have been grown on LaAlO$_3$(001) substrates by pulsed-laser deposition. Three types of ferroelectric capacitors, i.e., Pt/PZT/LSMO (A), LSMO/PZT/LSMO (B), and Pt/PZT/LSMO (C) have been fabricated, where the Pt electrode was sputter deposited onto as-grown (capacitor A) and *in situ* annealed (capacitor C) PZT/LSMO films, respectively. It is found that the LSMO/PZT/LSMO capacitor shows a low coercive field and good fatigue endurance up to 10^{10} switching cycles. Similar properties are also obtained for capacitor A. However, the capacitor C, with the PZT film *in situ* annealed at reduced oxygen pressures, exhibits higher switching voltages and starts to fatigue rapidly at about 10^6 bipolar switching cycles. Lead deficiency at the surface of the annealed PZT films has been observed. Our results demonstrate that the fatigue performance of PZT/LSMO films, although affected greatly by the electrode configurations, is intrinsically determined by the interface property at the top electrode. © *2000 American Institute of Physics.* [S0003-6951(00)02147-1]

Ferroelectric thin films have great potential for use in nonvolatile memories.[1] Among the many families of ferroelectrics, Pb(Zr, Ti)O$_3$(PZT) and their derivatives have been one of the most extensively studied materials due to their large remnant polarization (P_r) and low coercive field (E_c). However, PZT capacitors with noble metal electrodes like Pt exhibit a significant polarization fatigue when subject to bipolar switching pulses. To overcome this fatigue problem in PZT, the use of conducting oxide electrodes such as RuO$_2$, La$_{0.5}$Sr$_{0.5}$CoO$_3$, YBa$_2$Cu$_3$O$_y$, LaNiO$_3$, SrRuO$_3$, and IrO$_2$ have been reported.[2–7] It is believed that the oxygen vacancies in the PZT films can easily exchange with the oxygen in the oxide electrodes, thereby reducing the oxygen vacancy pileup at the interfaces and reducing the fatigue.[3,8] La$_{0.7}$Sr$_{0.3}$MnO$_3$(LSMO) is also a metallic oxide and has attracted great interest recently due to its colossal magnetoresistance.[9] When fully oxygenated, epitaxial LSMO films show a room-temperature resistivity of about 300 $\mu\Omega$ cm, comparable to those of the oxide electrodes mentioned previously.[10] In a previous report, we have shown that the LSMO films are very stable against postdeposition annealing at various oxygen pressures,[11] which distinguishes them from some other conductive oxide films like La$_{0.5}$Sr$_{0.5}$CoO$_3$.[12] LSMO/PZT/LSMO capacitors have not been studied.[13–15] In addition, recent results suggest that good fatigue endurance of PZT capacitors can be obtained if conducting oxides are used in both the top and bottom electrodes. The asymmetrical Pt (top)/PZT/oxide (bottom) and oxide/PZT/Pt capacitors, on the other hand, show substantial

fatigue.[2–4] However, according to Nakamura *et al.*, fatigue-free behavior up to 10^{12} cycles has been demonstrated on IrO$_2$/PZT/Pt capacitors.[16] Similar results were also reported for SrRuO$_3$/PZT/Pt and Pt/PZT/LSMO capacitors.[6,15] Clearly, to elucidate the fatigue phenomenon, these controversial observations need to be clarified.

In this work, epitaxial PZT/LSMO and LSMO/PZT/LSMO heterostructures were fabricated on LaAlO$_3$(LAO) substrates by pulsed-laser deposition (PLD). Three capacitor types of Pt/PZT/LSMO (A), LSMO/PZT/LSMO (B), and Pt/PZT/LSMO (C) with the Pt top electrode sputtered onto as-grown (capacitor A) and *in situ* annealed (capacitor C) PZT/LSMO films were fabricated. Structural and ferroelectric properties of these capacitors are evaluated. It is found that capacitor A shows a low E_c and good fatigue endurance up to 10^{10} cycles, comparable to the properties of the LSMO/PZT/LSMO capacitor. In contrast, capacitor C exhibits a higher E_c and starts to fatigue rapidly at about 10^6 cycles. We show that the fatigue behavior of PZT films, although affected by the electrode configurations, is basically controlled by the interface property at the top electrode.

The LSMO and PZT targets with compositions of La$_{0.7}$Sr$_{0.3}$MnO$_3$ and Pb(Zr$_{0.52}$Ti$_{0.48}$)O$_3$ were made by standard solid state reactions.[10,17] The PZT/LSMO and LSMO/PZT/LSMO heterostructures were grown on LAO(001) substrates by PLD using a 248 nm KrF excimer laser with a repetition rate of 10 Hz.[11] The laser energy density irradiated on the rotating LSMO and PZT targets was 6 and 3 J/cm^2, respectively. Both the LSMO and PZT films were deposited at 620 °C with the oxygen pressure fixed at 200 mTorr.[9,17] The top LSMO films were deposited *in situ* using a shadow

---
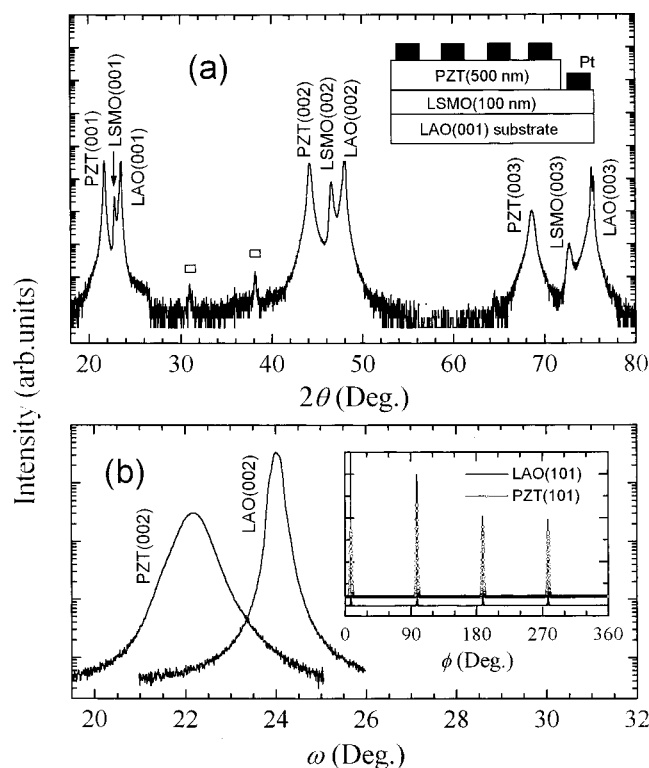
a)Electronic mail: wuwb@ustc.edu.cn

FIG. 1. Typical XRD profiles from the PZT/LSMO/LAO(001) heterostructures. (a) The specular linear scan along the normal of PZT(001) diffraction planes. The weak peaks at 30.88° and 38.14° may originate from the laser-produced particulates. (b) The ω-scan rocking curves on the PZT(002) and LAO(002) reflections. The ϕ scans on the PZT(101) and LAO(101) reflections are shown in the inset to (b). The inset to (a) shows a schematic illustration of the Pt/PZT/LSMO capacitors.

FIG. 2. Typical $P-E$ hysteresis loops measured from capacitor A (a), B (b), and C (c), as denoted. The data were taken at the maximum driving voltages of 2, 4, 6, 8, and 10 V.

mask with holes of 0.2 mm in diameter. After deposition, the PZT/LSMO and LSMO/PZT/LSMO films were cooled at 1 atm of oxygen. For comparison, some PZT/LSMO heterostructures were *in situ* annealed at 620 °C under 200 mTorr for 20 min before being cooled at 1 atm of oxygen. The thicknesses of the LSMO and PZT films are measured to be 100 and 500 nm, respectively. These films were structurally analyzed by x-ray diffraction (XRD), and x-ray photoemission spectroscopy (XPS). For the PZT/LSMO films, circular Pt top electrodes ($\varnothing = 0.2$ mm) were deposited *ex situ* through a shadow mask by sputtering at room temperature. The inset to Fig. 1(a) is a schematic diagram of the Pt/PZT/LSMO capacitors. The ferroelectric properties of the capacitors were measured using a RT66A standardized test system.

Figure 1(a) shows a XRD linear scan from a PZT/LSMO/LAO(001) heterostructure. It is seen that strong (00*l*) (*l* = 1, 2, and 3) reflections from each of the constituent layers were obtained. The weak peaks labeled with open squares can be assigned to the PZT(110) and PZT(111) reflections and may originate from the laser-produced particulates. All the layers were indexed according to a pseudocubic structure.[14] As shown in Fig. 1(b), XRD ω-scan rocking curves on the PZT(002) and LAO(002) reflections yielded a full width at half maximum of 0.63° and 0.35°, respectively, indicative of good crystallinity of the PZT film. XRD ϕ scans on the PZT(101) and LAO(101) reflections were also performed [the inset to Fig. 1(b)] and a parallel epitaxial relationship between the different layers was confirmed.

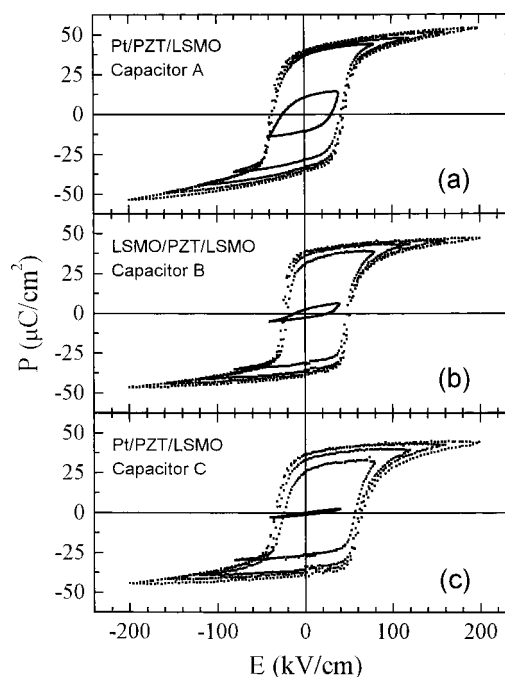Figure 2 shows the typical polarization versus electric-

field ($P-E$) loops recorded for capacitors A, B, and C. Capacitors A and C have the same electrode configuration but different thermal histories for the PZT/LSMO heterostructure. On the other hand, capacitors B and C have an almost identical thermal process for the PZT/LSMO but different top electrodes. The five loops represent the maximum driving voltages of 2, 4, 6, 8, and 10 V. They are quite symmetrical for capacitor A, but positively biased for capacitors B and C. The voltage shift means that an internal bias field has built up in the PZT films.[18] For all the capacitors, a large P_r was obtained. The P_r of capacitors A and B is almost saturated at a low driving voltage of 4 V. In contrast, capacitor C has a saturated P_r at a much higher voltage. For capacitors A, B, and C, the E_c at 6 V is calculated to be 38, 35, and 48 kV/cm, respectively. Note that capacitor C has a much larger E_c than capacitors A and B.

To further characterize the ferroelectric properties of the capacitors, we performed fatigue tests using bipolar square waves with maximum amplitude of 4–10 V at 25 kHz. Figures 3(a), 3(b), and 3(c) show the data measured from capacitors A, B, and C, respectively. In Fig. 3(a), although Pt was used as the top electrode, the capacitor shows no sign of loss of polarization after 10^9 cycles (closed circle). This fatigue-free behavior is very similar to that exhibited by the PZT film with symmetrical LSMO electrodes shown in Fig. 3(b). On the contrary, capacitor C starts to fatigue rapidly at about 10^6 cycles. The insets to Figs. 3(b) and 3(c) show the $P-E$ loops taken before (open square) and after (closed square) the fatigue tests on capacitors B and C, respectively. The fatigue behaviors observed for the different capacitors are found independent of the switching voltage amplitude and very reproducible for the capacitors having the same PZT/LSMO heterostructure. Clearly, the polarization loss is not solely determined by the electrode configuration.

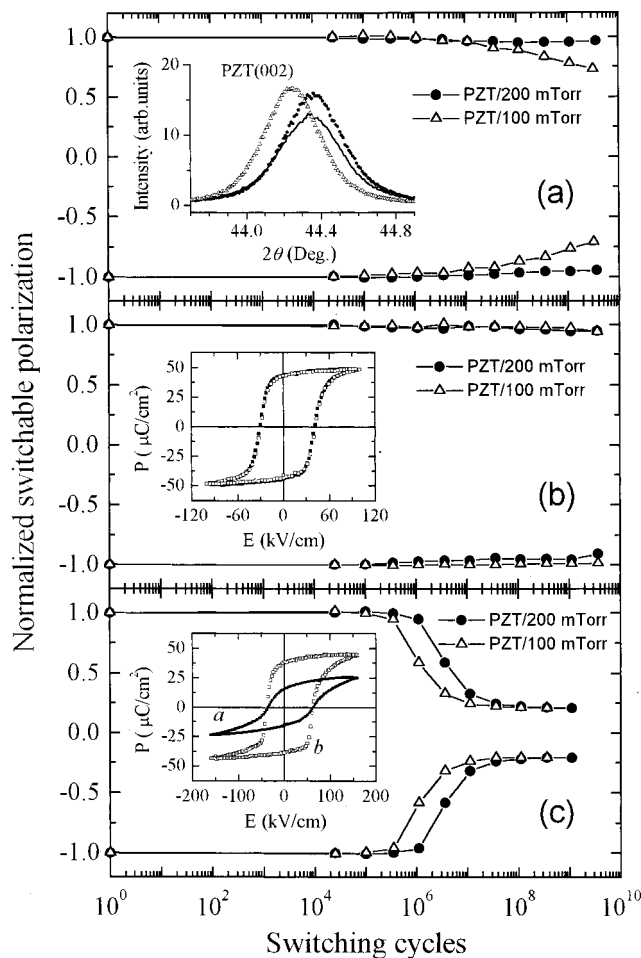We believe that after the *in situ* annealing, oxygen and

FIG. 3. Plots of normalized switchable polarization vs fatigue cycles at 25 Hz for capacitor A (a), B (b), and C (c). Note that the PZT layer was deposited at 200 (●) and 100 mTorr (△) of oxygen ambient, respectively. The inset to (a) shows PZT(002) reflections from the as-deposited (symbol) and *in situ* annealed (line) PZT/LSMO heterostructures. The insets to (b) and (c) show the $P-E$ loops before (□) and after (■) the fatigue tests.

lead loss may occur at the surface layer of the PZT films. After being cooled at 1 atm of oxygen, however, the oxygen content in the films should be recovered but the lead loss would be an irreversible process. In order to study the oxygen-content effect, we also deposited the PZT layer at a lower oxygen pressure of 100 mTorr. The inset to Fig. 3(a) shows PZT(002) peaks from as-grown PZT/LSMO heterostructures with the PZT layer grown at 200 (closed circle) and 100 mTorr (open triangle), respectively. The solid line represents the PZT(002) reflection from the *in situ* annealed PZT/LSMO film with the PZT layer grown at 200 mTorr. As the oxygen concentration is decreased, the PZT(002) reflection shifts to a lower Bragg angle, as expected.[19] The data in the inset to Fig. 3(a) also indicate that the oxygen content of the PZT films controlled during the deposition is not affected by the *in situ* annealing. The fatigue data on the capacitors with PZT grown at 100 mTorr are shown also in Figs. 3(a)– 3(c) (open triangle). Almost the same features are observed. Thus, the oxygen content in PZT films seems not to be the major factor responsible for the different fatigue performances observed. According to Cillessen *et al.*, due to the much smaller heat of formation and higher vapor pressure of PbO compared to TiO_2 and ZrO_2, desorption of PbO from

the PZT film will occur after annealing at the high temperature.[17] The lead loss is irreversible and may occur within a surface layer only of the PZT films under the annealing conditions. If lead deficiency occurs in the whole layer, the lattice constant and P_r value of the PZT film will change,[20] which is inconsistent with our observations. Indeed, XPS analyses on the Pb $4f$, Zr $3d$, and Ti $2p$ core-level spectra (not shown) reveal an average Pb/Zr mole ratio of 2.16 and 1.82 for the as-grown and annealed PZT/LSMO films, respectively, reflecting that lead deficiency did exist at the surface of the annealed PZT films. It is believed that the local compositional variations will induce point defects or a space-charge layer at the top Pt/PZT interface, and result in the high E_c and rapid fatigue observed for capacitor C. However, the use of all-oxide electrodes prevents such problems.[8,17] The substantial fatigue observed for the capacitor A [Fig. 3(a), open triangle] may also be ascribed to a lead loss at the PZT film surface, since the films were grown at a lower oxygen background pressure of 100 mTorr.

In summary, the epitaxial LSMO/PZT/LSMO capacitors show a low coercive field and good fatigue endurance up to 10^{10} bipolar switching cycles. For Pt/PZT/LSMO capacitors, switching and fatigue properties are found to be dependent on the thermal process of the PZT films. Our results indicate that the fatigue performance of PZT/LSMO films, although affected greatly by the electrode configurations, is basically controlled by the interface property at the top electrode.

[1] S. Sinharroy, H. Buhay, D. R. Lampe, and M. H. Francombe, J. Vac. Sci. Technol. A **10**, 1554 (1992).
[2] H. N. Al-Shareef, O. Auciello, and A. I. Kingon, J. Appl. Phys. **77**, 2146 (1995).
[3] M.-S. Chen, T.-B. Wu, and J.-M. Wu, Appl. Phys. Lett. **68**, 1430 (1996).
[4] R. Ramesh, W. K. Chan, B. Wilkens, H. Gilchrist, T. Sands, J. M. Tarascon, D. K. Fork, J. Lee, and A. Safari, Appl. Phys. Lett. **61**, 1537 (1992).
[5] R. Ramesh, H. Gilchrist, T. Sands, V. G. Keramidas, R. Haakenaasen, and D. K. Fork, Appl. Phys. Lett. **63**, 3592 (1993).
[6] I. Stolichnov, A. Tagantsev, N. Setter, J. S. Cross, and M. Tsukada, Appl. Phys. Lett. **74**, 3552 (1999).
[7] T. Nakamura, Y. Nakao, A. Kamisawa, and H. Takasu, Appl. Phys. Lett. **65**, 1522 (1994).
[8] J. J. Lee, C. L. Thio, and S. B. Desu, J. Appl. Phys. **78**, 5073 (1995).
[9] R. von Helmolt, J. Wecker, B. Holzapfel, L. Schultz, and K. Samwer, Phys. Rev. Lett. **71**, 2331 (1993).
[10] J. M. D. Coey, M. Viret, L. Ranno, and K. Ounadjela, Phys. Rev. Lett. **75**, 3910 (1995).
[11] W. Wu, K. H. Wong, X.-G. Li, C. L. Choy, and Y. H. Zhang, J. Appl. Phys. **87**, 3006 (2000).
[12] S. Madhukar, S. Aggarwal, A. M. Dhote, R. Ramesh, A. Krishnan, D. Keeble, and E. Poindexter, J. Appl. Phys. **81**, 3543 (1997).
[13] S. Mathews, R. Ramesh, T. Venkatesan, and J. Benedetto, Science **276**, 238 (1997).
[14] A. M. Grishin, S. I. Khartsev, and P. Johnsson, Appl. Phys. Lett. **74**, 1015 (1999).
[15] Q. Li, J. Yin, C. Xiao, and Z. Liu, J. Phys. D **33**, 107 (2000).
[16] T. Nakamura, Y. Nakao, A. Kamisawa, and H. Takasu, Jpn. J. Appl. Phys., Part 1 **33**, 5207 (1994).
[17] J. F. M. Cillessen, M. W. J. Prins, and R. M. Wolf, J. Appl. Phys. **81**, 2777 (1997).
[18] J. Lee, R. Ramesh, V. G. Keramidas, W. L. Warren, G. E. Pike, and J. T. Evans, Jr., Appl. Phys. Lett. **66**, 1337 (1995).
[19] Y. G. Zhao, M. Rajeswari, R. C. Srivastava, A. Biswas, S. B. Ogale, D. J. Kang, W. Prellier, Z. Chen, R. L. Greene, and T. Venkatesan, J. Appl. Phys. **86**, 6327 (1999).
[20] S. Aggarwal, S. Madhukar, B. Nagaraj, I. G. Jenkins, R. Ramesh, L. Boyer, and J. T. Evans, Jr., Appl. Phys. Lett. **75**, 716 (1999).